Tropical influence independent of ENSO on the austral summer Southern Annular Mode

Hui Ding[1], Richard J. Greatbatch[2], and Gereon Gollan[1]

Hui Ding, GEOMAR Helmholtz Centre for Ocean Research Kiel, Düsternbrooker Weg 20, 24105 Kiel, Germany. (hding@geomar.de)

[1]GEOMAR Helmholtz Centre for Ocean Research Kiel, Kiel, Germany

[2]GEOMAR Helmholtz Centre for Ocean Research Kiel and Kiel University, Kiel, Germany

This article has been accepted for publication and undergone full peer review but has not been through the copyediting, typesetting, pagination and proofreading process, which may lead to differences between this version and the Version of Record. Please cite this article as doi: 10.1002/2014GL059987

Abstract

A link between atmospheric variability in the Tropics independent of ENSO and the Southern Annular Mode (SAM) is found based on seasonal mean data for austral summer. Variations associated with El Niño Southern Oscillation (ENSO) are removed using a linear method and a Tropics Index (TI) is defined as the zonal average of the ENSO-removed 500 hPa geopotential height between $10°S$ and $10°N$. Since the detrended TI shows no link to SST variability in the Tropics, it appears to be related to internal atmospheric variability. We find that the TI can explain about 40% variance of the SAM interannual variability and about 75% of the SAM long term trend between 1957/58 and 2001/02, where here the SAM includes the ENSO signal. Positive/negative values of the TI are associated with the positive/negative SAM. A possible link between the TI and global warming is noted.

1. Introduction

The Southern Annular Mode (SAM) is the dominant mode of variability in the Southern Hemisphere atmospheric circulation and accounts for 20%-30% of the total monthly sea level pressure (SLP) or geopotential height variance south of 20°S [e.g., *Thompson and Wallace*, 2000]. The SAM is characterized by a dipole in geopotential height with opposing centers of action near 40° and 65°S and an equivalent barotropic structure in the vertical. There is a corresponding structure in the zonal wind field, with stronger southward-shifted westerly winds in the positive phase [e.g., *Thompson and Wallace*, 2000]. Numerous studies have noted the impact of the SAM on the Southern Hemisphere climate system [e.g., *Hall and Visbeck*, 2002; *Screen et al.*, 2009; *Lefebvre et al.*, 2004; *Stammerjohn et al.*, 2008]. Thus, it is of great socio-economic interest to study the variability of the SAM.

Many studies have reported the influence of tropical sea surface temperature (SST) variability on the Southern Hemisphere climate system [e.g., *Grassi et al.*, 2005; *Zhou and Yu*, 2004; *L'Heureux and Thompson*, 2006; *Ding et al.*, 2012]. For example, a negative/positive SAM index in summer is often associated with a warm/cold event in the tropical Pacific [e.g., *Zhou and Yu*, 2004; *Carvalho et al.*, 2005; *Ding et al.*, 2012]. *L'Heureux and Thompson* [2006] found that the extratropical signature of El Niño Southern Oscillation (ENSO) projects strongly onto the SAM during austral summer (defined as the months November-February) when roughly 25% of the temporal variability in the SAM is linearly related to fluctuations in ENSO over the period 1979/80 to 2003/04. *Ding et al.* [2012] found that the atmospheric response to tropical SST anomalies resembles the Pacific South American (PSA) pattern [*Karoly*, 1989] and projects strongly onto the SAM in the Pacific sector.

In addition, some studies suggest that tropical variability, independent of ENSO, can impact Southern Hemisphere climate [e.g., *Carvalho et al.*, 2005; *Ding et al.*, 2012]. Results from *Carvalho et al.* [2005] show that intraseasonal oscillations from the Tropics influence the SAM during austral summer (DJF), and *Ding et al.* [2012] noted an extratropical response in the Southern Hemisphere to tropical internal atmospheric variability on intraseasonal time scales in other seasons. *Yoo et al.* [2011, 2012] have also noted the impact of the Madden Julian Oscillation [*Madden and Julian*, 1994] on both the Antarctic and Arctic climates. However, it is not clear whether such influence exists based on seasonal mean data, an issue we investigate here. We are motivated at least partly by experiments using the ECMWF model, with relaxation to reanalysis in the Tropics, which suggest that tropical forcing independent of ENSO influences the seasonal mean SAM during austral summer, even before 1979 when the influence of ENSO on the SAM was weak (as discussed elsewhere).

2. Results

The results presented here are based mostly in the ERA-40 reanalysis [*Uppala et al.*, 2005] but with corroboration using the NCEP [*Kalnay et al.*, 1996] and ERA-Interim [*Dee et al.*, 2011] reanalysis products. We define the austral summer SAM as the first Empirical Orthogonal Function (EOF) of the austral summer (DJF) mean 500 hPa height (Z500) anomalies over the extratropical Southern Hemisphere (domain 30°S poleward). The SAM index is then the principal component time series of this EOF. Other definitions of the SAM have been employed using, respectively, 700 hPa height and sea level pressure (SLP) anomalies, but the time series are almost identical. Prior to the EOF analysis,

the seasonal DJF mean climatology has been removed to calculate anomalies, which are then weighted by the square root of cosine of latitude to provide equal weighting of equal areas, but no trend has been removed. EOFs have also been calculated using detrended data. The first EOF in this case has almost the identical spatial pattern to that obtained using undetrended data and the time series differ only by the trend (not shown). In the following, the EOFs using undetrended data are employed. Following *L'Heureux and Thompson* [2006], variations associated with ENSO are measured using the cold tongue index (CTI) defined as the anomaly in SST averaged over the region spanning 6°N-6°S, 180°-90°W.

The spatial patterns of the austral summer SAM and associated principal component (PC) time series are shown in Fig. 1. The SAM explains about 34% of the total variance in Z500 in the extratropical Southern Hemisphere summer. The CTI (inverted) is also shown in Fig. 1b. It is apparent that the positive/negative phase of the SAM is associated with La Niña/El Niño conditions (positive/negative in the inverted CTI) in the equatorial Pacific (Fig. 1b), consistent with previous studies [e.g., *Zhou and Yu*, 2004; *Carvalho et al.*, 2005; *L'Heureux and Thompson*, 2006; *Fogt and Bromwich*, 2006; *Ding et al.*, 2012], although the relationship is not stationary (Fig. 1b), being stronger after 1979. The SAM index displays a trend toward its positive phase in recent decades [e.g., *Thompson et al.*, 2000; *Thompson and Solomon*, 2002; *Ding et al.*, 2012]. The trend in the SAM has been attributed to forcing by stratospheric ozone depletion and increasing greenhouse gases [e.g., *Fyfe et al.*, 1999; *Thompson and Solomon*, 2002; *Gillett and Thompson*, 2003; *Marshall et al.*, 2004; *Shindell and Schmidt*, 2004; *Arblaster and Meehl*, 2006; *Miller*

et al., 2006; *Thompson et al.*, 2011]. Nevertheless, some recent studies have suggested that forcing from the Tropics played a role [*Ding et al.*, 2012; *Greatbatch et al.*, 2012].

Variations associated with ENSO (measured by the CTI) are removed from Z500 data using the linear method. The correlation pattern (after detrending; Fig. 2a) between the austral summer SAM index and the ENSO-removed Z500 anomalies is quite similar to the SAM spatial pattern in its positive phase (Fig. 1a), which is not surprising. What is more interesting is that the correlation shows an almost uniform positive correlation in the Tropics. It is notable that anomalously high/low Z500 (independent of ENSO) in the Tropics is associated with a positive/negative SAM index, contrary to the ENSO relationship with the SAM in which anomalously high/low Z500 in the Tropics is associated with a negative/positive SAM (as implied by Fig. 1b).

A Tropics Index (TI; Fig. 1c) is defined as the spatial average of the ENSO-removed Z500 anomaly over the tropical belt (0°E-360°E, 10°S-10°N; also see the black box in Fig. 2a). The TI does not correlate significantly with SST after detrending (not shown), indicating that it is associated primarily with internal atmospheric variability. We have also computed a Tropics Index in the same way using data from 850 hPa and 200 hPa. The correlation of the resulting detrended time series and that at 500 hPa is 0.77 and 0.7, respectively, significantly different from zero at the 99% level, and both indices, after detrending, show no significant connection to the underlying SST in the Tropics. Both indices also exhibit a very similar upward trend to that found at 500 hPa. Given these results, we use the index defined at 500 hPa for the following analysis.

It is clear from Fig. 1c that the TI shows some resemblance to the SAM index. In particular, the correlation between the TI and the SAM index is significantly different from zero at the 99% level (0.65 after detrending) over the period 1957/58 to 2001/02. Furthermore, the correlation pattern (after detrending; Fig. 2b) between the TI and full Z500 anomalies (including ENSO) is quite similar to the SAM spatial pattern in its positive phase (Fig. 1a), further indicating that the interannual variations associated with the TI in the extratropical Southern Hemisphere project onto the pattern associated with the SAM (Fig. 1a).

Another feature apparent from Figure 1c is that both the TI and the SAM index show upward trends. To investigate the link between the trends of the TI and the SAM index, we calculated the regression of Z500 anomalies (with ENSO retained) onto the TI (Fig. 1c) after detrending so that the regression reflects the link on interannual time scales. We then reconstruct variations in Z500 by multiplying the spatially varying regression coefficient by the TI, now including the trend, and then project the resulting fields onto the SAM pattern (30°S poleward) to produce a time series whose trend is shown in Figure 2c by the blue line. The trend of the SAM index (shown by the black line) is 0.4/(10years) while the trend of the SAM due to the TI is 0.3/(10years). It is therefore plausible that a large part of the positive trend in the SAM index is associated with the TI, an issue discussed further in the Summary and Discussion.

We now investigate the stability of the link between the SAM index and the TI on interdecadal time scales using running correlation analysis with a 21 year window. It is found that the link is stable during the ERA-40 period (blue line in Fig. 3). Using the

longer NCEP reanalysis for the above analysis corroborates the stable relationship during the ERA40 period but also shows a breakdown of the relationship prior to 1957/58 and post 2001/02 (red line in Fig. 3). The breakdown post 2001/02 is further confirmed by repeating the analysis using data from the ERA-Interim reanalysis (black line in Fig. 3). These results indicate a non-stationary relationship between the TI and the SAM, not unlike that between ENSO and the SAM, a topic for further investigation.

3. Summary and Discussion

In this study, we have investigated the influence of atmospheric variability in the Tropics, which is independent of ENSO, on the Southern Annular Mode (SAM) based on austral summer mean (seasonal mean over December/January/February, DJF) data. A linear method is employed to remove variations associated with ENSO (represented by the CTI (Fig. 1b)) from 500hPa geopotential height (Z500) anomalies. A Tropics Index (TI; Fig. 1c) is then defined as the spatial average of the ENSO-removed Z500 seasonal mean (DJF) anomalies within 10° of the equator. The detrended TI index does not correlate significantly with seasonal mean SST indicating that it is primarily associated with internal atmospheric variability in the Tropics, one possibility being the Madden Julian Oscillation (MJO) (see *Yoo et al.* [2011, 2012] for an illustration of how the MJO can affect high latitude climate). We found a significant link between the TI and the SAM (Fig. 1) on both interannual time scales and for explaining the long term trend. The TI can explain about 40% of the variance of the SAM interannual variability throughout the period 1957/58 to 2001/02. Furthermore, about 75% of the positive trend of the SAM index over this period can be explained by the Tropics index.

It should be noted that the link between the TI and the SAM is distinct and opposite from that between ENSO and the SAM. Both the TI and the inverted CTI (a measure of ENSO) are positively correlated with the SAM throughout the ERA-40 period. However, whereas positive anomalies of the TI are associated with warmer than normal conditions on interannual time scales in the tropical troposphere, positive anomalies of the inverted CTI are associated with colder than normal conditions (Figure 4). Similar opposing extratropical responses to heating in the Tropics have been noted by *Lu et al.* [2008] and *Sun et al.* [2013]. Relatively broad, upper tropospheric warming, such as associated with global warming, leads to an extratropical response similar to that identified here with the TI, and contrasts with the narrower, deeper heating associated with ENSO [*Sun et al.*, 2013]. Both extratropical responses are facilitated by eddies, the mechanism in the case of ENSO having been described by *Seager et al.* [2003] and in the case of global warming by *Lu et al.* [2014], with low level baroclinicity playing a role in the ENSO response [*Sun et al.*, 2013]. We hypothesize that the impact of increasing greenhouse gases on the positive trend of the SAM could be realized by means of the TI. It is also interesting to note the similarity between the temperature pattern associated with the TI and that associated with the SOM1 mode of variability that has been identified by *Lee and Feldstein* [2013] (compare Figure 4a with Figure 4a in *Lee and Feldstein* [2013]). SOM1 is an intraseasonal mode of variability that *Lee and Feldstein* [2013] suggest can occur more frequently under greenhouse gas forcing. A link between the trend in the TI and greenhouse gas forcing is, therefore, plausible.

Acknowledgments. This work has been funded by the BMBF MiKlip Project MODINI, by GEOMAR and by the DFG under ISOLAA, a project within the Priority Programme 1158. Data shown in this paper are available by email from corresponding author. We are grateful to two anonymous reviewers for their helpful comments on the paper and to Dr. Jian Lu for discussions that helped us clarify the distinction between the two different extratropical responses to tropical heating.

References

Arblaster, J. M., and G. A. Meehl (2006), Contributions of external forcings to southern annular mode trends, *J. Climate*, *19*(12), 2896–2905, doi:10.1175/JCLI3774.1.

Carvalho, L. M., C. Jones, and T. Ambrizzi (2005), Opposite phases of the Antarctic Oscillation and relationships with intraseasonal to interannual activity in the tropics during the austral summer, *J. Climate*, *18*(5), 702–718, doi:10.1175/JCLI-3284.1.

Dee, D., S. Uppala, A. Simmons, P. Berrisford, P. Poli, S. Kobayashi, U. Andrae, M. Balmaseda, G. Balsamo, P. Bauer, et al. (2011), The ERA-Interim reanalysis: Configuration and performance of the data assimilation system, *Quart. J. Roy. Meteor. Soc.*, *137*(656), 553–597, doi:10.1002/qj.828.

Ding, Q., E. J. Steig, D. S. Battisti, and J. M. Wallace (2012), Influence of the tropics on the Southern Annular Mode, *J. Climate*, *25*(18), 6330–6348, doi: http://dx.doi.org/10.1175/JCLI-D-11-00523.1.

Fogt, R. L., and D. H. Bromwich (2006), Decadal variability of the ENSO teleconnection to the high-latitude South Pacific governed by coupling with the Southern Annular Mode, *J. Climate*, *19*(6), 979–997, doi:10.1175/JCLI3671.1.

Fyfe, J., G. Boer, and G. Flato (1999), The Arctic and Antarctic Oscillations and their projected changes under global warming, *Geophys. Res. Lett.*, *26*(11), 1601–1604, doi: 10.1029/1999GL900317.

Gillett, N. P., and D. W. Thompson (2003), Simulation of recent Southern Hemisphere climate change, *Science*, *302*(5643), 273–275, doi:10.1126/science.1087440.

Grassi, B., G. Redaelli, and G. Visconti (2005), Simulation of polar Antarctic trends: Influence of tropical SST, *Geophys. Res. Lett.*, *32*(23), L23,806, doi:10.1029/2005GL023804.

Greatbatch, R. J., G. Gollan, and T. Jung (2012), An analysis of trends in the boreal winter mean tropospheric circulation during the second half of the 20th century, *Geophys. Res. Lett.*, *39*(13), 13,809, doi:10.1029/2012GL052243.

Hall, A., and M. Visbeck (2002), Synchronous Variability in the Southern Hemisphere Atmosphere, Sea Ice, and Ocean Resulting from the Annular Mode*, *J. Climate*, *15*(21), 3043–3057, doi:10.1175/1520-0442(2002)015<3043:SVITSH>2.0.CO;2.

Kalnay, E., M. Kanamitsu, R. Kistler, W. Collins, D. Deaven, L. Gandin, M. Iredell, S. Saha, G. White, J. Woollen, et al. (1996), The NCEP/NCAR 40-Year Reanalysis Project, *Bull. Am. Meteorol. Soc.*, *77*(3), 437–471, doi:10.1175/1520-0477(1996)077¡0437:TNYRP¿2.0.CO;2.

Karoly, D. J. (1989), Southern hemisphere circulation features associated with El Niño-Southern Oscillation events, *J. Climate*, *2*(11), 1239–1252, doi:10.1175/1520-0442(1989)002<1239:SHCFAW>2.0.CO;2.

Lee, S., and S. B. Feldstein (2013), Detecting ozone-and greenhouse gas–driven wind trends with observational data, *Science*, *339*(6119), 563–567, doi:

10.1126/science.1225154.

Lefebvre, W., H. Goosse, R. Timmermann, and T. Fichefet (2004), Influence of the Southern Annular Mode on the sea ice–ocean system, *J. Geophys. Res.*, *109*(C9), 9005, doi: 10.1029/2004JC002403.

L'Heureux, M. L., and D. W. Thompson (2006), Observed relationships between the El Niño-Southern Oscillation and the extratropical zonal-mean circulation, *J. Climate*, *19*(2), 276–287, doi:10.1175/JCLI3617.1.

Lu, J., G. Chen, and D. M. Frierson (2008), Response of the zonal mean atmospheric circulation to El Niño versus global warming, *J. Climate*, *21*(22), 5835–5851, doi: http://dx.doi.org/10.1175/2008JCLI2200.1.

Lu, J., L. Sun, Y. Wu, and G. Chen (2014), The role of subtropical irreversible PV mixing in the zonal mean circulation response to global warming-like thermal forcing, *J. Climate*, *27*(6), 22972316, doi:http://dx.doi.org/10.1175/JCLI-D-13-00372.1.

Madden, R. A., and P. R. Julian (1994), Observations of the 40-50-day tropical oscillation-A review, *Mon. Wea. Rev.*, *122*(5), 814–837, doi:10.1175/1520-0493(1994)122<0814:OOTDTO>2.0.CO;2.

Marshall, G. J., P. A. Stott, J. Turner, W. M. Connolley, J. C. King, and T. A. Lachlan-Cope (2004), Causes of exceptional atmospheric circulation changes in the Southern Hemisphere, *Geophys. Res. Lett.*, *31*(14), 14,205, doi:10.1029/2004GL019952.

Miller, R., G. Schmidt, and D. Shindell (2006), Forced annular variations in the 20th century intergovernmental panel on climate change fourth assessment report models, *J. Geophys. Res.*, *111*(D18), D18,101, doi:10.1029/2005JD006323.

Rayner, N., D. Parker, E. Horton, C. Folland, L. Alexander, D. Rowell, E. Kent, and A. Kaplan (2003), Global analyses of sea surface temperature, sea ice, and night marine air temperature since the late nineteenth century, *J. Geophys. Res.*, *108*(D14), 4407–4453, doi:10.1029/2002JD002670.

Screen, J. A., N. P. Gillett, D. P. Stevens, G. J. Marshall, and H. K. Roscoe (2009), The role of eddies in the Southern Ocean temperature response to the Southern Annular Mode, *J. Climate*, *22*(3), 806–818, doi:10.1175/2008JCLI2416.1.

Seager, R., N. Harnik, Y. Kushnir, W. Robinson, and J. Miller (2003), Mechanisms of Hemispherically Symmetric Climate Variability., *J. Climate*, *16*(18), 2960–2978, doi:10.1175/1520-0442(2003)016<2960:MOHSCV>2.0.CO;2.

Shindell, D. T., and G. A. Schmidt (2004), Southern Hemisphere climate response to ozone changes and greenhouse gas increases, *Geophys. Res. Lett.*, *31*(18), L18,209, doi:10.1029/2004GL020724.

Stammerjohn, S., D. Martinson, R. Smith, X. Yuan, and D. Rind (2008), Trends in Antarctic annual sea ice retreat and advance and their relation to El Niño–Southern Oscillation and Southern Annular Mode variability, *J. Geophys. Res.*, *113*(C3), 3, doi:10.1029/2007JC004269.

Sun, L., G. Chen, and J. Lu (2013), Sensitivities and Mechanisms of the Zonal Mean Atmospheric Circulation Response to Tropical Warming., *J. Atmos. Sci.*, *70*(8), 2487–2504, doi:10.1175/JAS-D-12-0298.1.

Thompson, D. W., and S. Solomon (2002), Interpretation of recent Southern Hemisphere climate change, *Science*, *296*(5569), 895–899, doi:10.1126/science.1069270.

Thompson, D. W., and J. M. Wallace (2000), Annular modes in the extratropical circulation. Part I: month-to-month variability*, *J. Climate*, *13*(5), 1000–1016, doi:10.1175/1520-0442(2000)013<1000:AMITEC>2.0.CO;2.

Thompson, D. W., J. M. Wallace, and G. C. Hegerl (2000), Annular modes in the extratropical circulation. Part II: Trends, *J. Climate*, *13*(5), 1018–1036, doi:10.1175/1520-0442(2000)013<1018:AMITEC>2.0.CO;2.

Thompson, D. W., S. Solomon, P. J. Kushner, M. H. England, K. M. Grise, and D. J. Karoly (2011), Signatures of the Antarctic ozone hole in Southern Hemisphere surface climate change, *Nature Geosci*, *4*(11), 741–749, doi:10.1038/ngeo1296.

Uppala, S., P. Kållberg, A. Simmons, U. Andrae, V. Bechtold, M. Fiorino, J. Gibson, J. Haseler, A. Hernandez, G. Kelly, et al. (2005), The ERA-40 re-analysis, *Quart. J. Roy. Meteor. Soc.*, *131*(612), 2961–3012, doi:10.1256/qj.04.176.

Yoo, C., S. Feldstein, and S. Lee (2011), The impact of the Madden-Julian Oscillation trend on the Arctic amplification of surface air temperature during the 1979–2008 boreal winter, *Geophys. Res. Lett.*, *38*(24), 24,804, doi:10.1029/2011GL049881.

Yoo, C., S. Lee, and S. Feldstein (2012), The impact of the Madden-Julian oscillation trend on the Antarctic warming during the 1979–2008 austral winter, *Atmospheric Science Letters*, *13*(3), 194–199, doi:10.1002/asl.379.

Zhou, T., and R. Yu (2004), Sea-surface temperature induced variability of the Southern Annular Mode in an atmospheric general circulation model, *Geophys. Res. Lett.*, *31*(24), L24,206, doi:10.1029/2004GL021473.

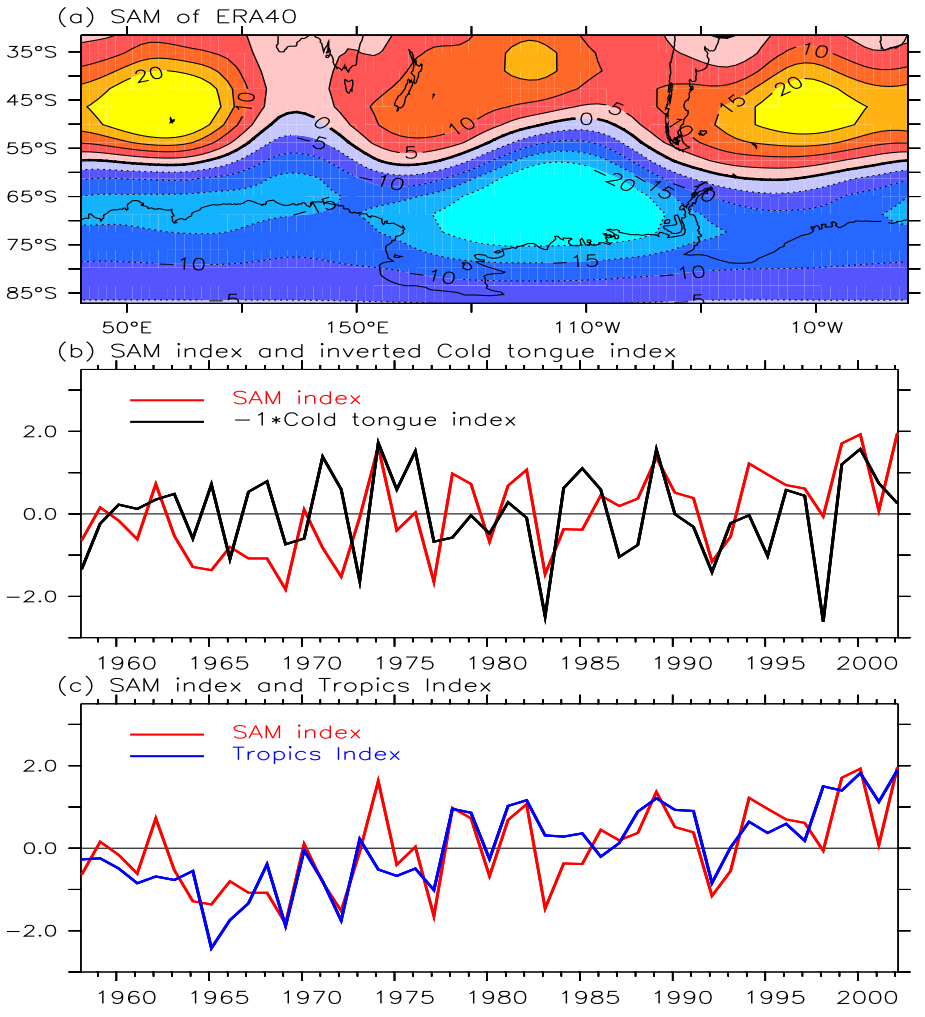

Figure 1. Spatial pattern (a) and time series (b) of the austral summer Southern Annular Mode (SAM) from ERA40 (1957/58 - 2001/02). The spatial pattern shows the Z500 anomaly corresponding to one standard deviation positive of the index which, in turn, has been normalised by its standard deviation. Also shown in panel (b) is the inverted cold tongue index (CTI) defined using HadISST data (*Rayner et al.* [2003]). Panel (c) shows the Tropics Index (TI), defined as in the text, together with the SAM index from panel b.

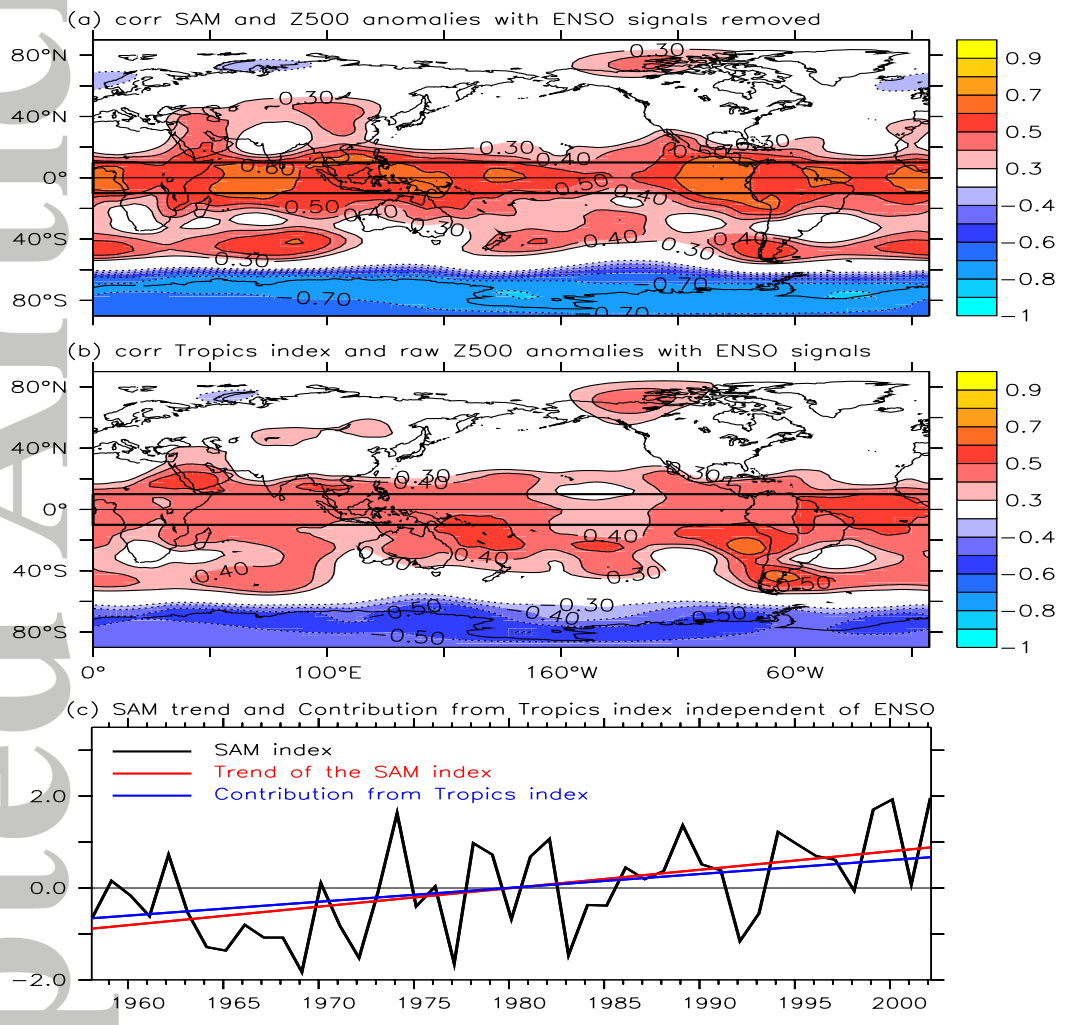

Figure 2. (a) Correlation between the SAM index (see Fig. 1) and Z500 anomalies with ENSO removed; (b) correlation between the TI and Z500 anomalies with ENSO included; and (c) the SAM index. (c) also shows the trend of the SAM index (red line) and the SAM trend derived from the TI, as described in the text. In panels a and b, detrended data are used for the analysis.

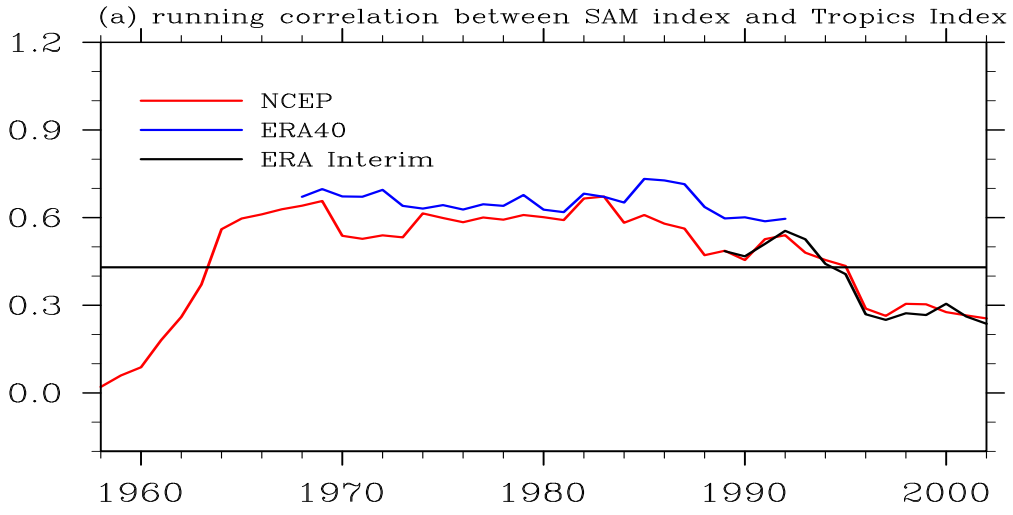

Figure 3. Correlation between the SAM index and the TI (both detrended) in running 21 year windows computed using the NCEP (red line; *Kalnay et al.* [1996]), ERA40 (blue line; *Uppala et al.* [2005]) and ERA Interim (black line; [*Dee et al.*, 2011]) reanalyses. The horizontal black line indicates the 95% significance level.

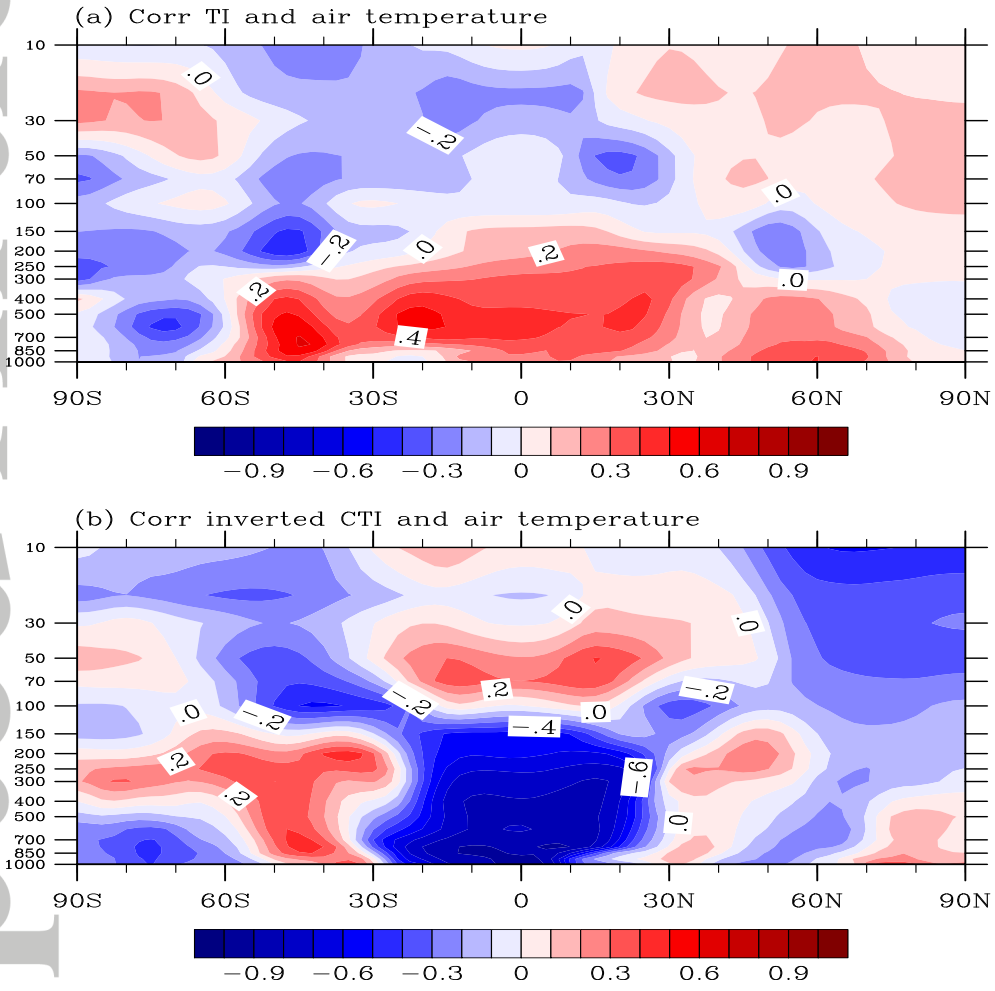

Figure 4. Correlation between seasonal mean (DJF) zonally-averaged temperature and (a) the TI and (b) the inverted CTI (all time series detrended). The contour interval is 0.1.